JOURNAL OF OPTOELECTRONICS AND ADVANCED MATERIALS Vol. 9, No. 5, May 2007, p. 1516 - 1520

The ferroectric-electric characterization of PZT-PbS composites

V. STANCU[a], M. BUDA[a], L. PINTILIE[b,*], M. POPESCU[a*], F. SAVA[a]
[a] *National Institute of Materials Physics Bucharest-Magurele, P. O. Box MG-7, 77125, Romania*
[b] *Max Planck Institute of Microstructure Physics, Weinberg 2, Halle, 06129 Germany*

A new method for the preparation of PbS/PZT composite materials is proposed. The PZT matrix has been obtained using the sol-gel method on Pt-coated Si substrates. The PbS (nano) crystals were subsequently obtained by dipping the porous PZT matrix in $Pb(NO_3)_2$ and Na_2S solutions at room temperature. The XRD spectra show the presence of the tetragonal phase of PZT. The microstructure of the film was analyzed using scanning electron microscopy (SEM) and atomic force microscopy (AFM). The size of the PbS (nano)-particles at the sample's surface is about 25 nm, estimated from the AFM analysis. The roughness of the sample's surface is about 5 nm. The porosity of the composite, estimated from the SEM analysis in cross-section is smaller than for the reference PZT porous matrix. The equivalent dielectric constant of the composite increases by a factor of 4-5 in comparison with the porous PZT reference and does not depend on the thickness of the surface PbS (nano)-crystalline layer. The saturated polarization (Ps) value for the PZT-PbS composite is smaller than that corresponding to the bulk PZT but higher than for the reference porous PZT. We attribute these effects to the partial filling of the pores in the PZT matrix with PbS.

(Received November 14, 2006; accepted April 12, 2007)

Keywords: Composite PZT-PbS, Sol-gel, Dipping

1. Introduction

Semiconductor nanocrystals received recently a large attention due to their application in non-linear optics, especially in transparent media [1]. Many authors have predicted for nanoparticle semiconductors enhanced nonlinearities resulting from quantum confinement effects [2,3]. The most studied nanocrystalline semiconductors belong to II-VI and IV-VI groups, as particles or in thin film form. The representative semiconductor for the IV-VI group is the lead sulfide (PbS), a material widely used to manufacture infrared (IR) detectors for the wavelength domain up to 4 μm as its band-gap is about 0.41 eV at room temperature and 0.29 eV at liquid-N_2 temperature, respectively. In the last years PbS nanoparticles were successfully grown, by chemical methods, in various dielectric matrix such as polymer, glass or glass-ceramic [4,5].

The Chemical Solution Deposition (CSD), known also as the sol-gel method, is a comfortable way for the preparation of ferroelectric thin films, especially $PbZr_xTi_{1-x}O_3$ (PZT) [6-8]. As it is known, the PZT in bulk or thin film form posses very good pyroelectric properties, which make this material very attractive for applications such as non-contact temperature measurements, fire and intruders alarms, gas sensing, or thermal imaging [9-11]. Like PbS, the PZT-made pyroelectric detectors are used for the IR domain. The difference is that the PbS detectors are photonic-type, working on the photo-resistive effect, while the PZT-made detectors are thermal-type, working on the pyroelectric effect [12,13]. This is the reason why the responsivity of a PbS detector is wavelength dependent, while that of a PZT-pyroelectric detector is wavelength independent. The response of a pyroelectric detector is the same for wavelengths up to 15 μm if the power of the incident radiation is constant. Considering these aspects, it would be interesting to combine the two compounds and to investigate the electric and photoelectric properties of the resulting material.

The first step would be the preparation of the composite. The fastest way is to prepare a porous PZT matrix by using the sol-gel method and to insert PbS nanoparticles into the pores by using the dipping method. This paper presents the preparation method of the PZT-PbS composite films on platinized silicon (Pt/Si) substrates. The dielectric and ferroelectric properties were investigated and discussed. It will be shown that the presence of the PbS nanoparticles in the PZT film leads to a change of the ferroelectric properties compared with the reference porous and dense PZT samples.

2. Experimental

PZT porous films were prepared by the sol-gel method. The PZT precursor solution were prepared from lead acetate $Pb(CH_3COO)_2*3H_2O$ (Reactivul Bucuresti), zirconium n-propoxide $Zr[O(CH_2)_2CH_3]_4$ (Alfa) and titanium isopropoxide Ti $[OCH(CH_3)_2]_4$ (Alfa) dissolved 2-methoyethanol (Aldrich). The solution contains 5 wt % excess of lead precursor and has a Zr/Ti ratio of 20/80. The porosity was induced by the addition 7 wt % of

polyvinilpyrrolidone (PVP) into the PZT stock solution. The PZT porous films were deposited on platinized silicon substrate (Pt/TiO_2 /SiO_2/Si) by spin – coating at 3000 rpm for 30 s, followed by pyrolisis at 200 ^oC/2 min and 350 ^oC/3 min. After six coatings, the crystallization of the porous PZT matrix was performed by Conventional Thermal Annealing (CTA) at 650 ^oC/30 min, with a heating rate of 5 °C/ min. More details about the deposition pocess are given in Ref. 14.

PbS (nano)-crystals were prepared by dipping the porous PZT films, first into a 1M lead nitrate [$Pb(NO_3)_2$] aqueous solution (dipping time 30 sec or 60 sec), and then in a 0.5 M aqueous solution of sodium sulfide (Na_2S), with the same dipping time. The PbS is formed by the sulfuration of the Pb^{2+} ions adsorbed on the surface and in the pores of the PZT film after dipping in the first solution. This procedure will be colled "one layer of PbS". The completed composite was annealed at two different temperatures, of 100 ^oC and 200 ^oC, respectively (see Table 1). This final annealing is necessary on one hand to eliminate the residual water from the composite, and on the other hand has the role to sensitize the PbS nano-particles. It is known that the photo-sensitivity of the chemically deposited PbS increases very much after annealing long time, at moderate temperature, in air [15,16].

Table 1. Deposition conditions of the PZT-PbS composite films.

Sample	Compositions	Substrate	Number of deposited layers	Annealing condition (final) of PZT- PbS structure
III	PZT - PbS	Pt/Si	1 layer PbS (30s)	200 ^oC/ 30 min
IV	PZT - PbS	Pt/Si	3 layers PbS (30s)	200 ^oC/ 30 min
V	PZT - PbS	Pt/Si	3 layers PbS (30s)	200 ^oC/ 15 min
VI	PZT - PbS	Pt/Si	3 layers PbS (60s)	200 ^oC/ 15 min
VII	PZT - PbS	Pt/Si	3 layers PbS (30s)	100 ^oC/ 15 min
VIII	PZT - PbS	Pt/Si	3 layers PbS (60s)	100 ^oC/ 15 min

The crystalline phases of composite films were identified by X-ray diffraction (XRD) in θ-2θ geometry. The microstructure of the films was investigated by scanning electron microscopy (SEM) and atomic force microscopy (AFM). Gold electrodes were deposited by thermal evaporation through a shadow mask onto the surface of the PZT-PbS composite films. Values of the dielectric constant (ε_r) were estimated from the room temperature capacitance-voltage (C-V) characteristics obtained with an Agilent LCR meter at a frequency of 1kHz. P-E hysteresis loops were also obtained using a RT 66A Analyzer at 100 Hz and room temperature.

3. Results and discussion

Fig. 2 shows XRD patterns of PZT - PbS films and dense PZT on Pt-coated Si substrate. The PZT dense film shows predominant tetragonal perovskite phase. The perovskite structure of PZT films was emphasized by the splitting of the (001)/ (100), (002)/(200) peaks. The presence of PbS is evidenced by (111), (200), (220) peaks. The intensity of the PbS peaks is very small. This observation is correlated with the fact that the presence of the PbS nano-particles was evidenced by the SEM analysis only in a thin surface layer (≈ 50 nm) on top of the porous PZT film. This PbS doped layer is much thinner than the total thickness of the PZT matrix (more than 300 nm).

The surface microstructure of the PZT porous matrix and PZT-PbS composites deposited on Pt/Si substrates is shown in Fig. 3. The SEM analysis showed a crack-free surface, not very smooth porous microstructure. Table 3 presents the final thickness of the porous films measured in cross-section by scanning electron microscopy (SEM) on a freshly fractured surface.

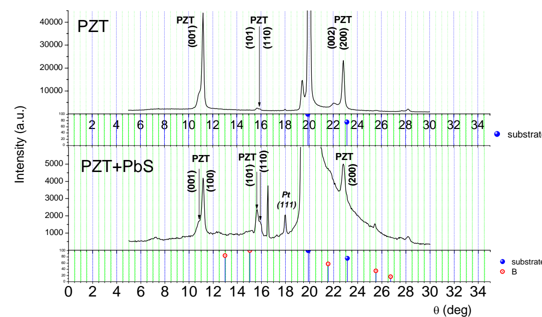

Fig. 2. X-ray diffraction patterns of PZT –PbS and dense PZT films.

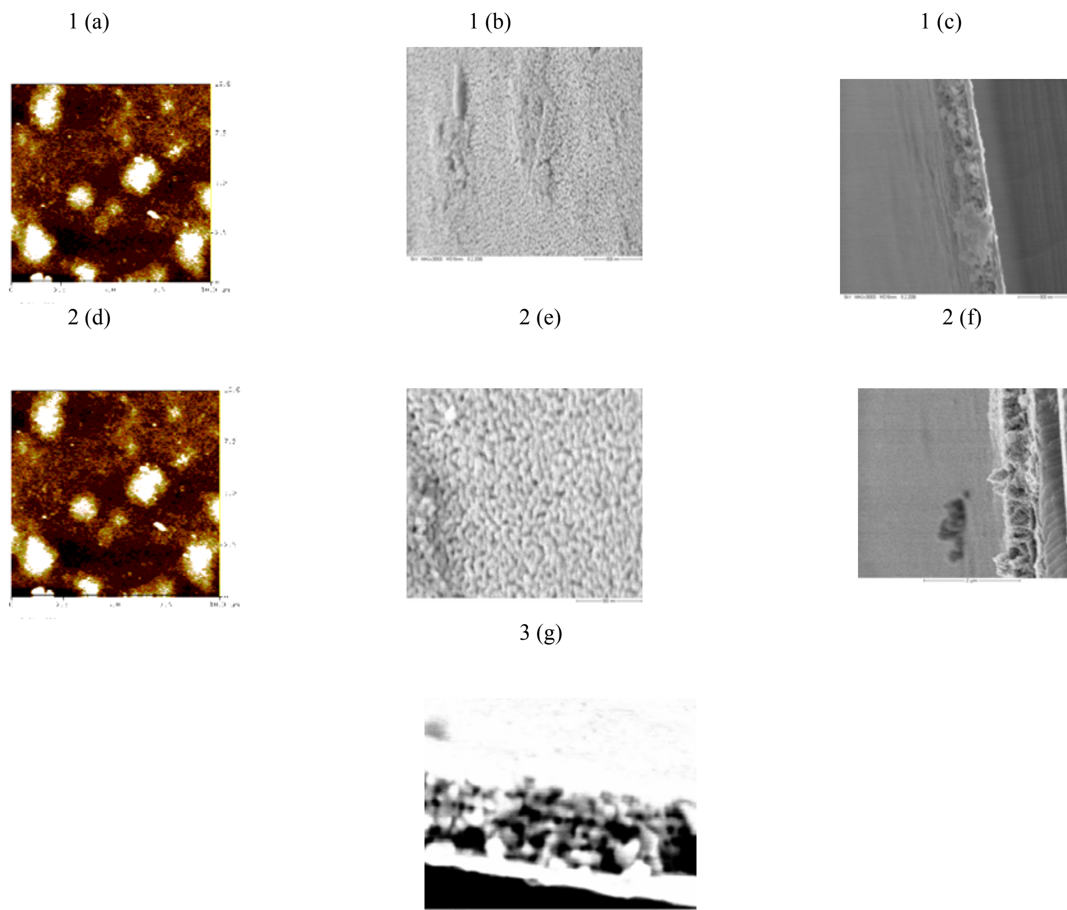

Fig. 3. Morphological analysis of the PZT-PbS samples. 1- PZT-PbS composite annealed at 200 ^{o}C/ 15 min, AFM image (a), surface SEM image (b), and cross-section SEM image (c). 2 – PZT-PbS composite annealed at 100 ^{o}C/ 15 min, AFM image (d), surface SEM image (e), and cross-section SEM image (f). 3 – initial porous PZT matrix, cross-section SEM image (g).

The thickness of the PZT porous matrix is larger than that of the dense PZT layer, obtained without the addition of the PVP polymer. Although this effect cannot be used directly to estimate the porosity, it is related to the presence of the pores. The cross-sectional SEM analysis does not show directly the presence of PbS in the pores of the PZT matrix. We have to have in mind though that for quantum size nano-particles SEM is not the optimum analysis technique because of its poor resolution. What is evident from the SEM analysis is that the initial porous PZT matrix has larger pores than the PZT-PbS composite films, possibly due to the partial filling of the PZT pores with PbS (nano)-particles.

The cross-sectional SEM analysis also shows very clearly the presence of a quasi-continuous ultra-thin layer (about 50 nm) on top of the PZT porous matrix, with a characteristic grain size of 25 nm. This layer is not present in the reference PZT matrix and we associate it to the deposition of a PbS (nano)-crystalline thin layer on the top of the PZT matrix after the dipping process.

The AFM roughness analysis has shown that the surface roughness of the PZT-PbS films deposited on Pt/Si is about 5 nm for the sample with final heat treatment at 200 ^{o}C. For the sample with final heat treatment at 100 ^{o}C we observed an increased surface roughness, up to 15 nm.

The hysteresis loops obtained at the frequency of 100 Hz are presented in the Figure 5 for the dense PZT and PZT-PbS films deposited on Pt/Si substrate. Table II summarizes the results. The remnant polarization (P_r) of the dense PZT film is higher than for the porous PZT matrix or the PZT-PbS composites. The values of the saturated polarization (P_s) for the PZT-PbS composite, lies between that of the dense PZT and that of the porous matrix. This behavior can be directly correlated with the smaller porosity of the PbS-PZT composites, possibly due to partial filling of the pores in the matrix with PbS. Further studies are needed in order to make clear the way in which porosity and the presence of PbS in the composite material affect the ferroelectric properties: remnant polarization, saturated polarization and coercive field. In the first instance it can be assumed that the replacement of the air in the pores, which has a low dielectric constant and is insulating, with PbS, which has a high dielectric constant (161) and is semiconductor,

contributes to a better compensation of the polarization charges. That leads to a partial de-pinning of the ferroelectric domains from the pores surface. The result is an increase in the polarization values.

From the C-V curves (Fig. 6), the zero field relative permittivity of porous PZT film, dense PZT film and PZT-PbS films were calculated using the model of a plan parallel capacitor. The obtained values are given in Table III. For the composite samples with PbS, the values of the dielectric constant ε = 250 are similar for samples V and VI (final annealing treatment 200 ^{o}C and different thickness of the PbS layer). Also, similar values for the dielectric constant, ε= 182, are found for samples VII and VII (final annealing treatment 100 ^{o}C and different thickness of the PbS layer). The thickness of the top PbS layer was controlled by the dipping time (see the Table 1).

The above observation suggests that the effect of the top PbS layer is very small and does not influence the equivalent dielectric constant of the composite material. In fact the structure can be regarded as serial connection of two capacitors, one is formed by the top ultra-thin PbS layer, the other is formed by the thicker porous PZT matrix doped with PbS in the pores. As the dielectric constant of PbS is 161 [17], comparable with that of the dense PZT, the capacitance of the ultra-thin PbS layer will be very large compared with that of the PbS-doped porous PZT film. Therefore, the equivalent capacitance of the serial capacitor connection will be practically equal with the capacitance of the PbS-doped porous PZT film. The presence of the PbS in the pores of the PZT matrix might play the important role in this case, considering the fact that the dielectric constants of the PbS-doped films is much larger than that of the not-doped porous PZT matrix, which is only is 48.

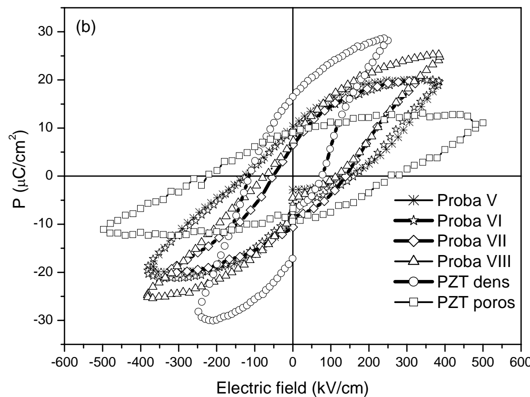

Fig. 5. P-E hysteresis loops at 100 Hz and room temperature.

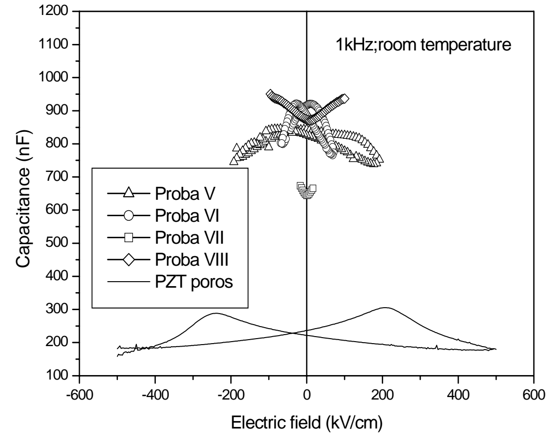

Fig. 6. C-V curves for all samples at room temperature and 1kHz.

Table 2. The average remnant polarization (P_{rm}) and coercive field (E_{cm}) for porous PZT, dense PZT and PZT-PbS samples.

Sample	P_{rm} (μC/cm^2)	E_{cm} (kV/cm)
V	10.8	133.65
VI	8.77	145
VII	7.56	96.99
VIII	7.95	96.4
Dense PZT	28.65	163
Porous PZT	9.2	250

Table 3. The dielectric constant and geometrical dimensions of the PZT porous matrix, PZT dense film and ferroelectric-semiconductor composite material.

Sample	C(pF) 20°C, 0V, 1kHz	d (nm)	S (mm^2)	ε_{film}
V	835	520	0.2	245
VI	907	500	0.2	256
VII	645	600	0.2	182
VIII	645	500	0.2	183
Dense PZT	15430	250	1.5	246
Porous PZT	1480	430	1.5	48

4. Conclusions

We have presented a new method for the preparation of ferroelectric-semiconductor PZT-PbS composite thin-films, by combining the sol-gel method used for the deposition of the porous PZT matrix and the dipping method for the deposition of PbS (nano)-particles on top and in the pores of the PZT matrix. The XRD analysis

shows the presence of the tetragonal phase of PZT and of crystalline PbS. Although the presence of the PbS nano-particles in the pores of the PZT matrix was not directly evidenced by the SEM analysis, the partial filling of the pores with PbS is suggested by the reduced porosity and by the results of the electric-ferroelectric measurements. Especially the dielectric constant values, which are very different for the non-doped and PbS-doped porous PZT films, suggest that PbS nano-particles are present in the structure after dipping and final annealing. The enhancement of the ferroelectric properties, evidenced by the hysteresis loop measurements, also suggest the presence of the semiconductor PbS in the structure.

Further studies are needed in order to investigate the possible charge transfer between PbS nano-particles and the ferroelectric PZT matrix and its IR properties.

Acknowledgement

This work was performed in the CERES 4-252 "FENAPOFS" project financed by the Romanian Ministry of Education and Research.

References

[1] R. Reisfeld, "New Materials for Nonlinear Optics", Optical and Electronic Phenomena in Sol-Gel Glasses and Modern Applicationjs, Eds. R. Reisfeld, C. K. Jorgensen, Structure and Bonding, 85, Springer-Verlang, 99-147, (1996).
[2] P. H. Roussingnol, D. Ricard, C. H. R. Flytzanis, Appl. Phys. **B51**, 437 (1990).
[3] H. Minti, M. Eyal, R. Reisfeld, G. Berkovic, Chem. Phys. Lett. 183, 277, (1991).
[4] R. Konenkamp, P. Hoyer, A. Wahi, J. Appl. Phys. **79**(9), 7029-7035, (1996).
[5] E. V. Nicolaeva et al., Materilas Science and Engineering C 8-9, 217-223, (1999).
[6] J. Zeng, C. Lin, K. Li, J. Li, Appl. Phys. A **69**, 93 (1999).
[7] V. S. Kumar, Y. Ohya, Y. Takahashi, Jpn. J. Appl. Phys, **37** (8), 4477-4481 (1998).
[8] K. D. Budd, S. K. Dey, D. A. Payne, Brit. Ceram. Proc. **36**, 107 (1985).
[9] R. W. Whatmore, Rep. Prog. Phys. **49**, 1335, (1986).
[10] V. Ferrari, D. Marioli, A. Taroni, E. Ranucci, Sens. Actuators B **68**, 81(2000).
[11] H. D. Chen, K. R. Udaykumar, C. J. Gaskey, L. E. Cross, J. Am. Ceram. Soc. **79**, 2189 (1996).
[12] J. N. Humphrey, Appl. Optics **4**, 665 (1965).
[13] L. Pintilie, M. Lisca, M. Alexe, Appl. Phys. Lett. **86**(19), 192902 (2005).
[14] V. Stancu, M. Lisca, I. Boerasu, L. Pintilie, M. Kosec, in press.
[15] E. Pentia, L. Pintilie, I. Matei, T. Botila, I. Pintilie, Infrared Physics and Technology **44**, 207 (2003).
[16] I. Pintilie, E. Pentia, L. Pintilie, D. Petre, T. Botila, C. Constantin, J. Appl. Phys. **78** (1), 1713 (1995).
[17] L. Pintilie, E. Pentia, I. Matei, I. Pintilie, J. Appl. Phys. **91**(9), 5782 (2002).

*Corresponding author: pintilie@mpi-halle.de